Phenomenological study of $\Omega_c \to \Omega^- \pi^+$ at polarized electron-positron collider

Yunlu Wang (王云路)[1†] Yunlong Xiao (肖云龙)[1‡] Pengcheng Hong (洪鹏程)[2,3§]

[1]Key Laboratory of Nuclear Physics and Ion-beam Application (MOE) and Institute of Modern Physics, Fudan University, Shanghai, China 200433
[2]College of Physics, Jilin University, Changchun, China 130012
[3]Institute of High Energy Physics, Beijing 100049

Abstract: The exploration of symmetry laws stands as a cutting-edge direction in modern physics research. This work delves into the examination of P and CP symmetry properties within the charm quark system by analyzing asymmetry parameters in the two-body decay process of Ω_c. By accounting for the polarization effects of electron and positron beams and employing the helicity formalism, we systematically analyze the decay characteristics of Ω_c and its subsequent hyperon decays through specific asymmetry parameters. A comprehensive formulation of the angular distribution for these decay processes has been developed. The research assesses the detection sensitivity of asymmetry parameters in the $\Omega_c \to \Omega^- \pi^+$ decay mode across different experimental conditions, including varying data sample sizes and beam polarization configurations. These results contribute to enriching a theoretical foundation for forthcoming experimental endeavors at the STCF, offering significant implications for symmetry studies in the charm sector.

Keywords: Beam polarization, Symmetry, Baryon, Sensitivity

DOI: 10.1088/1674-1137/ae6311 **CSTR:**

I. INTRODUCTION

The observed matter-antimatter asymmetry of the universe remains one of the most compelling puzzles in modern physics. While the Big Bang should have produced equal amounts of matter and antimatter, cosmological observations unequivocally show a universe dominated by matter. This indicates that there must be a mechanism in the evolution of the universe that favors matter over antimatter. Charge parity (CP) violation is one of Sakharov's three essential conditions for understanding the matter and anti-matter asymmetry in the universe [1]. In the Standard Model of particle physics, the quark dynamics are described by the Cabibbo-Kobayashi-Maskawa (CKM) mechanism [2, 3]. This theoretical framework was experimentally confirmed through a series of landmark measurements. The BaBar and Belle collaborations reported the observation of indirect CP violation in the decay of B mesons [4, 5] in 2001. Subsequently, the direct violation was observed during the rare decay process of B mesons [6, 7]. The first CP violation in the charm system was observed by LHCb collaboration in 2019 [8]. Recent LHCb results have significantly expanded the experimental landscape, with evidence of CP violation in $\Lambda_b \to \Lambda K^+ K^-$ [9] and the first observation in $\Lambda_b \to pK^-\pi^+\pi^-$ decays [10]. Similar searches of Λ, Σ^+, Ξ^0, and Ξ^- decays have also been performed by BESIII collaboration [11−16]. However, all CP measurements are not sufficient to explain the difference between matter and antimatter. The search for new CP-violating mechanisms has thus become a central focus in particle physics, driving both theoretical innovations and next-generation experiments [17].

Theoretically, the decay amplitude of Ω_c consists of factorizable and non-factorizable contributions. While non-factorizable contributions are typically negligible in charmed meson decays, Ω_c decays exhibit unique dynamics, as their amplitudes can receive contributions from both W-emission and W-exchange diagrams. The W-exchange diagram (manifesting as a pole diagram) escapes helicity and color suppression, leading to non-trivial contributions. In the case of W-exchange processes, which can be represented as pole diagrams, the typical suppression mechanisms related to helicity and color no longer apply [18]. As a result, theoretical predictions for charmed baryon decays tend to be more complex com-

Received 27 September 2025; Accepted 20 April 2026

† E-mail: yunluwang20@fudan.edu.cn
‡ E-mail: xiaoyunlong@fudan.edu.cn(Corresponding author)
§ E-mail: hongpc@ihep.ac.cn

pared to those for charmed mesons. Various theoretical frameworks have been developed to study these decays, such as the covariant confined quark model [19–21], the pole model [18, 22, 23], and current algebra [18, 23, 24]. The Cabibbo-favored decay $\Omega_c \to \Omega^-\pi^+$ is dominated by the W-emission process and also has a relatively large branching fraction, which makes it particularly interesting for studying parity (P) and CP violation. In Ω_c and $\bar{\Omega}_c$ two-body decays, the asymmetry parameters α_{Ω_c} and $\alpha_{\bar{\Omega}_c}$ quantify the contributions of P-wave (parity-violating) and D-wave (parity-conserving) amplitudes [25]. Specifically, α_{Ω_c} and $\alpha_{\bar{\Omega}_c}$ parameterize the decays of baryons and anti-baryons, where non-zero $\alpha_{\Omega_c}(\alpha_{\bar{\Omega}_c})$ and $(\alpha_{\Omega_c}+\alpha_{\bar{\Omega}_c})/(\alpha_{\Omega_c}-\alpha_{\bar{\Omega}_c})$ values mean P and CP violations. These features make Ω_c decays an ideal laboratory for symmetry test and polarization study, which can be explored at next-generation facilities. The Super Tau-Charm Facility (STCF) is designed to achieve a peak luminosity of 10^{35} cm^{-2}s^{-1} [26], representing a two-order-of-magnitude improvement over BESIII. With a center-of-mass energy range spanning $2-7$ GeV, which covers the production threshold for $\Omega_c\bar{\Omega}_c$ baryon pairs, STCF will enable unprecedented statistics for studies of charmed baryons. Recent theoretical studies have demonstrated that transverse and longitudinal beam polarization can improve parameter measurement precision at electron-positron colliders [27, 28].

In this work, we present a systematic investigation of how beam polarization affects Ω_c polarization by comparing with polar and azimuthal angle distributions of particles from Ω_c decay. We provide the first study of parameter sensitivity under different transverse and longitudinal polarization configurations. Furthermore, we evaluate the optimization effects of beam polarization schemes on CP violation. These phenomenological results establish crucial theoretical support to understand Ω_c decay at future STCF.

II. ANGULAR PARAMETERS

The decays in this analysis are described in a helicity formalism [29]. The helicity angles and amplitudes of the $\Omega_c\bar{\Omega}_c$ production and the decay of Ω_c are listed in Table 1, while the corresponding angles are shown in Fig. 1. The momenta p_i are obtained by boosting particle i to the rest frame of its mother particle, and the values of angles

Table 1. Helicity angles and amplitudes in relative decays.

decay	helicity angle	helicity amplitude
$\gamma^* \to \Omega_c(\lambda_1)\bar{\Omega}_c(\lambda_0)$	(θ_1,ϕ_1)	A_{λ_1,λ_0}
$\Omega_c(\lambda_1) \to \Omega^-(\lambda_2)\pi^+$	(θ_2,ϕ_2)	B_{λ_2}
$\Omega^-(\lambda_2) \to \Lambda(\lambda_3)K^-$	(θ_3,ϕ_3)	F_{λ_3}
$\Lambda(\lambda_3) \to p(\lambda_4)\pi^-$	(θ_4,ϕ_4)	H_{λ_4}

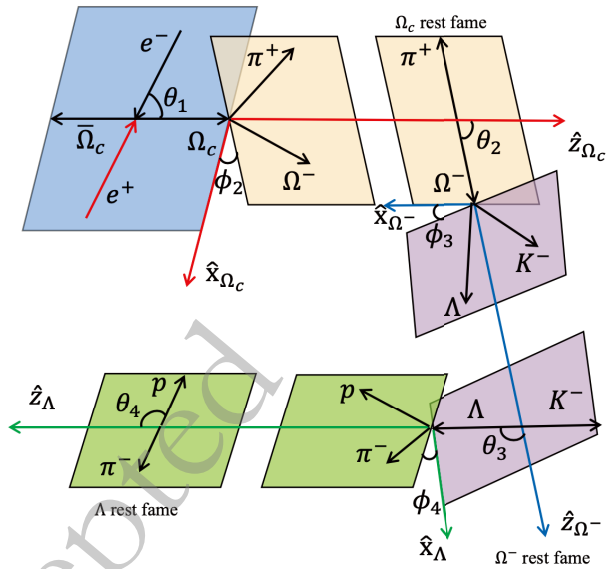

Fig. 1. (color online) Definition of helicity angles at e^+e^- collider.

can be constructed by the momenta.

In general, a helicity amplitude for a two-body decay process can be denoted by $A^J_{\lambda_i,\lambda_j}$, where J denotes the spin of the mother particle, and λ_i,λ_j are daughter particles' helicity values which are the projection of particle spin in momentum direction. Under parity conservation, the amplitudes will obey

$$A^J_{\lambda_i,\lambda_j} = \eta\eta_i\eta_j(-1)^{J-s_i-s_j}A^J_{-\lambda_i,-\lambda_j}, \tag{1}$$

where η_i is the intrinsic parity of each particle. The spins of the two daughter particles are denoted by s_i, s_j respectively.

For the first process in Table 1, the helicity values can be $\lambda_1 = \pm\frac{1}{2}$ and $\lambda_0 = \pm\frac{1}{2}$ for spin-$\frac{1}{2}$ particles Ω_c and $\bar{\Omega}_c$. The photon has spin $J=1$ and parity $\eta=1$, while the charmed baryons have $\eta_1=\eta_0=1$ and $s_1=s_0=\frac{1}{2}$. For simplification, the superscript J is suppressed in the following so that $A_{\lambda_i,\lambda_j} = A^J_{\lambda_i,\lambda_j}$. The other amplitudes B, F and H listed in Table 1 follow a similar notation. We also suppress the subscripts corresponding to the daughter particles $\pi^\pm$ and K^- such as $B_{\lambda_2} = B_{\lambda_2,0}$, since they are spin-zero particles.

If all processes in Table 1 are parity conserved, the corresponding helicity amplitudes, A, B, F, H satisfy following relations:

$$\begin{aligned} &A_{\frac{1}{2},\frac{1}{2}} = A_{-\frac{1}{2},-\frac{1}{2}}, A_{\frac{1}{2},-\frac{1}{2}} = A_{-\frac{1}{2},\frac{1}{2}}, \\ &B_{\frac{1}{2}} = -B_{-\frac{1}{2}}, F_{\frac{1}{2}} = -F_{-\frac{1}{2}}, H_{\frac{1}{2}} = -H_{-\frac{1}{2}}. \end{aligned} \tag{2}$$

Here, the scripts are suppressed if they are fixed constants. Specifically, since angular momentum conserva-

tion, only helicity values $\lambda_2 = \pm\frac{1}{2}$ of Ω^- are allowed, which leads to two amplitudes $B_{\pm\frac{1}{2}}$. In Standard Model, the P violations in weak decays make the above equations invalid. To quantify the violations, we define the following three asymmetric parameters:

$$\alpha_{\Omega_c} \equiv \frac{|B_{\frac{1}{2}}|^2 - |B_{-\frac{1}{2}}|^2}{|B_{\frac{1}{2}}|^2 + |B_{-\frac{1}{2}}|^2}, \tag{3}$$

$$\alpha_{\Omega^-} \equiv \frac{|F_{\frac{1}{2}}|^2 - |F_{-\frac{1}{2}}|^2}{|F_{\frac{1}{2}}|^2 + |F_{-\frac{1}{2}}|^2}, \tag{4}$$

$$\alpha_{\Lambda} \equiv \frac{|H_{\frac{1}{2}}|^2 - |H_{-\frac{1}{2}}|^2}{|H_{\frac{1}{2}}|^2 + |H_{-\frac{1}{2}}|^2}. \tag{5}$$

They are equivalent to original definitions from Lee-Yang [25] by decomposing amplitudes into S and P waves. The measured values of the last two parameters are $\alpha_{\Omega^-} = 0.0154 \pm 0.002$ [30] and $\alpha_{\Lambda} = 0.746 \pm 0.008$ [31], while the value of the parity parameter $\Omega_c \to \Omega^-\pi^+$ is still lack.

Moreover, if CP conservation holds in charge conjugate decay $\bar{\Omega}_c \to \Omega^+\pi^-$, the parity parameter of this decay is expected to have the same absolute value but an opposite sign, like $\alpha_{\bar{\Omega}_c} = -\alpha_{\Omega_c}$. Thus the CP violation can be characterized by

$$\mathcal{A}_{CP} \equiv \frac{\alpha_{\Omega_c} + \alpha_{\bar{\Omega}_c}}{\alpha_{\Omega_c} - \alpha_{\bar{\Omega}_c}}. \tag{6}$$

This definition has an advantage that the systematic uncertainties of production and detection asymmetries are largely cancelled [32]. The approximation of the parameter can be written by [15, 33]

$$\mathcal{A}_{CP} \propto -\tan\Delta\delta \tan\Delta\phi, \tag{7}$$

after inserting partial amplitudes. The relative strong phase $\Delta\delta$ predominantly arises from final-state interactions, which are discussed and computed within QCD factorization framework [34, 35] and resonance-induced model [36] for B decays. The weak phase $\Delta\phi$ stems from interference between amplitudes with different partial wave configurations in the same decay [37]. The amplitudes partially derive from tree and penguin diagrams like the examples shown in Fig. 2, where the tree diagram is Cabibbo-favored and the penguin diagram is suppressed from off-diagonal elements $V_{cb}^* V_{ts}^*$. The magnitude of the weak phase shift is determined by $\mathrm{Im}[-(V_{cb}^* V_{tb} V_{ts}^* V_{ud})]$ and expected at order of $O(10^{-4} \sim 10^{-5})$, which is close to predicted CP violation of hyperons systems [33, 38]. However, an additional

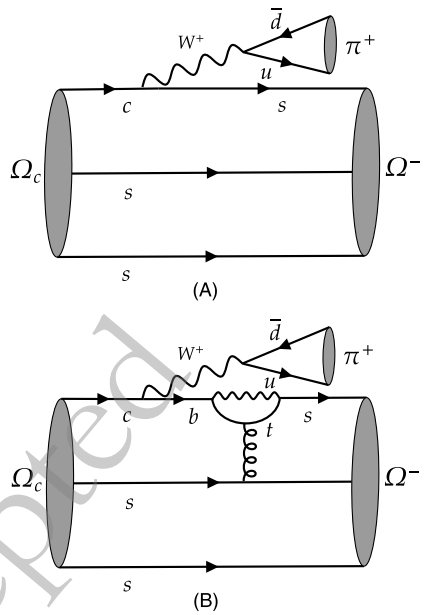

Fig. 2. Tree and penguin diagrams as examples for $\Omega_c \to \Omega^-\pi^+$ decay.

suppression of order 10^{-5} arises from the extra Fermi constant G_F in the penguin diagram when the partial waves in Ref. [39] are incorporated. Consequently, the observable CP violation in Eq. (6) is subject to further suppression. Including the direct CP violation, a greater number cannot be ruled out for the mixing of strong violation and even new physics, that demands performing measurements at future e^+e^- collider.

III. SPIN DENSITY MATRIX AND ANGULAR DISTRIBUTION

A. Ω_c production at e^+e^- collider

The density matrix (SDM) [40, 41] involves the spin and polarization information of particles. The SDM of spin-$\frac{1}{2}$ particles like Ω_c is expressed by a 2×2 matrix:

$$\rho^{\Omega_c} = \frac{\mathcal{P}_0}{2}\begin{pmatrix} 1+P_z & P_x - iP_y \\ P_x + iP_y & 1-P_z \end{pmatrix}, \tag{8}$$

where $\mathcal{P}_0$ carries the unpolarized information, while the information of transverse polarization is taken by $\mathcal{P}_x$ and $\mathcal{P}_y$. Operator $\mathcal{P}_z$ is longitudinal polarization. The information of initial collision is included by SDM of the virtual photon ρ^{γ^*}, which connects to ρ^{Ω_c} via the equation:

$$\rho^{\Omega_c}_{\lambda_1,\lambda_1'} = \sum_{\lambda,\lambda_0} \rho^{\gamma^*}_{\lambda,\lambda'} D^{1*}_{\lambda,\lambda_1-\lambda_0}(\phi_1,\theta_1,0) \times D^{1}_{\lambda',\lambda_1'-\lambda_0}(\phi_1,\theta_1,0) A_{\lambda_1,\lambda_0} A^*_{\lambda_1',\lambda_0}, \tag{9}$$

where $D^J_{\lambda_j,\lambda_k}$ is the Wigner-D function. For polarized symmetric e^+e^- beams, when the transverse and longitudinal polarizations are considered simultaneously, the SDM of polarized photon is given by [28]

$$\rho^{\gamma^*}_{\lambda,\lambda'} = \frac{1}{2}\begin{pmatrix} (1-p_L)(1+\bar{p}_L) & 0 & p_T^2 \\ 0 & 0 & 0 \\ p_T^2 & 0 & (1+p_L)(1-\bar{p}_L) \end{pmatrix}. \tag{10}$$

In a positron-electron annihilation experiment with symmetric beam energy, the electron and positron share the same transverse polarization p_T respecting the z axis, which is chosen along the positron momentum shown in Fig. 1. The longitudinal polarizations of electron is represented by factor p_L, and the ratio of the number of right-handed and left-handed electrons in the beam is determined by the factor through $(1+p_L)/(1-p_L)$, while another factor $\bar{p}_L$ is for positron. The diagonal elements indicate the fact that the photon couples either a single right-handed particle to a left-handed antiparticle or a single left-handed particle to a right- handed antiparticle.

We clarify the magnitude and phase angle of an amplitude by denoting $A_{\lambda_1,\lambda_0} = a_1 e^{i\zeta_1}$ and define the phase difference $\Delta_1 = \zeta_1 - \zeta_1'$. The other amplitudes take similar decompositions. Substituting Eq. (9) into Eq. (8) under parity conservation of Ω_c production, we get the unpolarized section which depends on the polarizations of the virtual photon, that is

$$\mathcal{P}_0 = (1-p_L\bar{p}_L)(1+\alpha_c\cos^2\theta_1) + p_T^2\alpha_c\sin^2\theta_1\cos 2\phi_1 . \tag{11}$$

Here constant $\frac{1}{2}|A_{\frac{1}{2},-\frac{1}{2}}|^2 + |A_{\frac{1}{2},\frac{1}{2}}|^2$ is suppressed, since it does not contribute to the final cross sections after normalization. The angular distribution parameter α_c for this production is defined by

$$\alpha_c \equiv \frac{|A_{\frac{1}{2},-\frac{1}{2}}|^2 - 2|A_{\frac{1}{2},\frac{1}{2}}|^2}{|A_{\frac{1}{2},-\frac{1}{2}}|^2 + 2|A_{\frac{1}{2},\frac{1}{2}}|^2}, \tag{12}$$

that has not been measured yet. In the following content, since the electromagnetic interaction is dominated for the production of the charged pair, we use hypothetical values $\alpha_c = 0.7$ and $\Delta_1 = \pi/6$, which are close to the measurements of strange baryons [42]. Our analysis framework is applicable to any value of α_c, and the actual value can be measured via the angular distribution of event number given in Eq. (20).

The transverse and longitudinal polarizations of Ω_c are

$$\begin{aligned}
\mathcal{P}_x &= \frac{\sqrt{1-\alpha_c^2}\sin\theta_1[(p_L-\bar{p}_L)\cos\Delta_1 - p_T^2\sin\Delta_1\sin 2\phi_1]}{1+\alpha_c\cos^2\theta_1 + p_T^2\alpha_c\sin^2\theta_1\cos 2\phi_1}, \\
\mathcal{P}_y &= \frac{\sqrt{1-\alpha_c^2}\sin\Delta_1\sin\theta_1\cos\theta_1(1-p_L\bar{p}_L - p_T^2\cos 2\phi_1)}{1+\alpha_c\cos^2\theta_1 + p_T^2\alpha_c\sin^2\theta_1\cos 2\phi_1}, \\
\mathcal{P}_z &= \frac{(1+\alpha_c)(\bar{p}_L - p_L)\cos\theta_1}{1+\alpha_c\cos^2\theta_1 + p_T^2\alpha_c\sin^2\theta_1\cos 2\phi_1}.
\end{aligned} \tag{13}$$

These polarizations reduce to the results in Ref. [28] when the incoming beams are polarized transversely, and turn to the expressions in Ref. [43] when electron beam is polarized longitudinally. For continuity and simplicity, we also treat the longitudinal polarization of positron beam to be zero by taking $\bar{p}_L = 0$. We have found that the dependences of results below on longitudinal beam polarizations are dominated by the difference $p_L - \bar{p}_L$. The $\cos\theta_1$ distribution of $\mathcal{P}_y$ can be obtained after integrating out ϕ_1, and its magnitude is improved by transverse polarization p_T as plotted in Fig. 3. Since the existence of polarized beams, the polarizations $\mathcal{P}_x$ and $\mathcal{P}_z$ are no longer flat, and the $\cos\theta_1$ distribution of $\mathcal{P}_z$ is shown in Fig. 4. The distribution of magnitude $|\mathcal{P}_{\Omega_c}| = \sqrt{\mathcal{P}_x^2 + \mathcal{P}_y^2 + \mathcal{P}_z^2}$ is also shown in Fig. 5, which highlights discernible differences associated with different beam polarization configurations.

B. Two-body decays and joint angular distributions

The information of P violation of this two-body decay is carried by the SDM of Ω^-, which is given by the relation

$$\rho^{\Omega^-}_{\lambda_2,\lambda_2'} \propto \sum_{\lambda_1,\lambda_1'} \rho^{\Omega_c}_{\lambda_1,\lambda_1'} D^{\frac{1}{2}*}_{\lambda_1,\lambda_2}(\phi_2,\theta_2) \times D^{\frac{1}{2}}_{\lambda_1',\lambda_2'}(\phi_2,\theta_2) B_{\lambda_2} B_{\lambda_2'}, \tag{14}$$

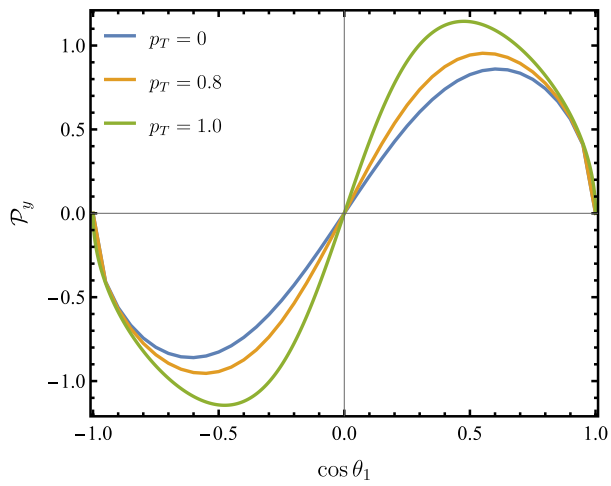

Fig. 3. (color online) The $\cos\theta_1$ distributions of polarization $\mathcal{P}_y$ for different transverse polarizations of beams. Here $p_L = 0$ is used.

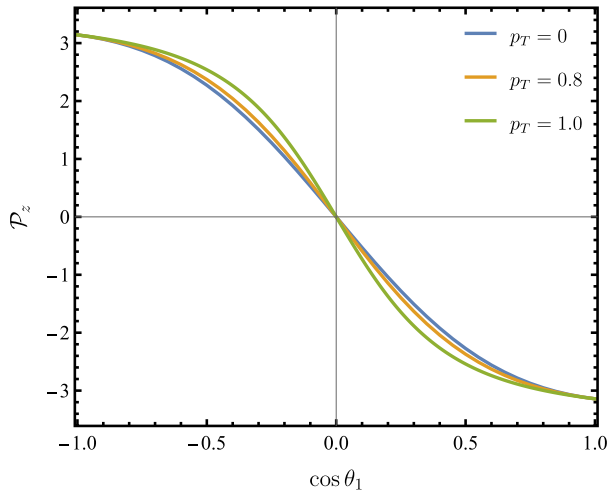

Fig. 4. (color online) The $\cos\theta_1$ distributions of polarization $\mathcal{P}_z$ for different transverse polarizations of beams. Here $p_L = 0.5$ is used.

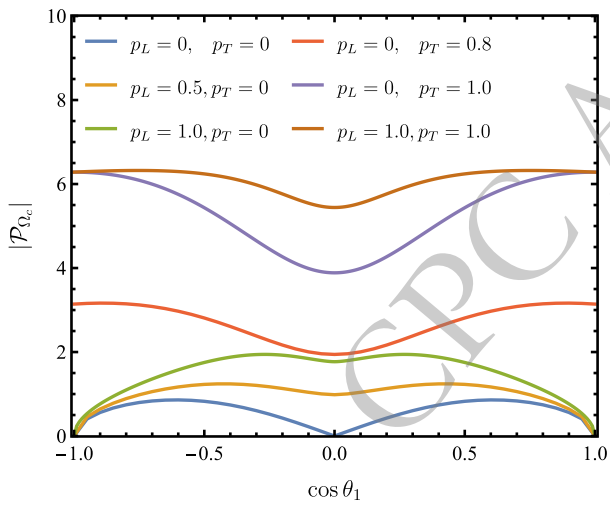

Fig. 5. (color online) Magnitudes of the Ω_c polarization as a function of $\cos\theta_1$ for different beam polarizations.

here the helicity value λ_2 or λ_2' is either $1/2$ or $-1/2$, that means the SDM ρ^{Ω^-} is also a 2×2 matrix likes Eq. (8). Then after summing all combinations and implementing simplifications, the unpolarized and longitudinal-polarized operators of Ω^- reduce to

$$\mathcal{P}_0^{\Omega^-} = \frac{2\mathcal{P}_0}{1+\alpha_{\Omega_c}}\left[1+\alpha_{\Omega_c}\cos\theta_2\mathcal{P}_z + \alpha_{\Omega_c}\sin\theta_2\left(\cos\phi_2\mathcal{P}_x+\sin\phi_2\mathcal{P}_y\right)\right], \tag{15}$$

$$\mathcal{P}_0^{\Omega^-}\mathcal{P}_z^{\Omega^-} = \frac{2\mathcal{P}_0}{1+\alpha_{\Omega_c}}\left\{\alpha_{\Omega_c}+\cos\theta_2\mathcal{P}_z + \sin\theta_2\left(\cos\phi_2\mathcal{P}_x+\sin\phi_2\mathcal{P}_y\right)\right\}, \tag{16}$$

and the transverse-polarized operators are

$$\mathcal{P}_0^{\Omega^-}\mathcal{P}_x^{\Omega^-} = \mathcal{P}_0\sqrt{\frac{1-\alpha_{\Omega_c}}{1+\alpha_{\Omega_c}}}\left\{\sin\Delta_2\left(\mathcal{P}_y\cos\phi_2-\mathcal{P}_x\sin\phi_2\right) - \cos\theta_2\left[\mathcal{P}_z\sin\theta_2-\left(\mathcal{P}_x\cos\phi_2+\mathcal{P}_y\sin\phi_2\right)\right]\right\}, \tag{17}$$

$$\mathcal{P}_0^{\Omega^-}\mathcal{P}_y^{\Omega^-} = \mathcal{P}_0\sqrt{\frac{1-\alpha_{\Omega_c}}{1+\alpha_{\Omega_c}}}\left\{\cos\Delta_2\left(\mathcal{P}_y\cos\phi_2-\mathcal{P}_x\sin\phi_2\right) + \sin\theta_2\left[\mathcal{P}_z\sin\theta_2-\left(\mathcal{P}_x\cos\phi_2+\mathcal{P}_y\sin\phi_2\right)\right]\right\}. \tag{18}$$

Finally, all parity information is compiled in the SDM of proton, which is expressed by

$$\rho^p_{\lambda_4,\lambda_4'} \propto \sum_{\lambda_1,\lambda_1'}\rho^{\Omega_c}_{\lambda_1,\lambda_1'}B_{\lambda_2}B_{\lambda_2'}F_{\lambda_3}F_{\lambda_3'}H_{\lambda_4}H_{\lambda_4'} \times D^{\frac{1}{2}*}_{\lambda_1,\lambda_2}(\phi_2,\theta_2)D^{\frac{1}{2}*}_{\lambda_2,\lambda_3}(\phi_3,\theta_3)D^{\frac{1}{2}*}_{\lambda_3,\lambda_4}(\phi_4,\theta_4) \times D^{\frac{1}{2}}_{\lambda_1',\lambda_2'}(\phi_2,\theta_2)D^{\frac{1}{2}}_{\lambda_2',\lambda_3'}(\phi_3,\theta_3)D^{\frac{1}{2}}_{\lambda_3',\lambda_4'}(\phi_4,\theta_4). \tag{19}$$

The polarizations of proton can be obtained using similar expressions of Eqs. (15)-(18) iteratively, and we suppress the explicit expressions here. The joint angular distribution is given by unpolarized section of proton $\mathcal{W} = \mathrm{Tr}\rho^p = \mathcal{P}_0^p$. The angular distribution of event number N for each angle is obtained by integrating out other angles, and the nontrivial distributions are

$$\frac{dN}{d\cos\theta_1} \propto 1+\alpha_c\cos^2\theta_1, \tag{20}$$

$$\frac{dN}{d\cos\theta_3} \propto 1+\alpha_{\Omega_c}\alpha_{\Omega^-}\cos\theta_3, \tag{21}$$

$$\frac{dN}{d\cos\theta_4} \propto 1+\alpha_{\Omega^-}\alpha_\Lambda\cos\theta_4, \tag{22}$$

$$\frac{dN}{d\phi_1} \propto 1+\frac{\alpha_c}{3}\left(1+2p_T^2\cos 2\phi_1\right), \tag{23}$$

$$\frac{dN}{d\phi_2} \propto 1+\frac{3\pi^2}{16}\alpha_{\Omega_c}\frac{\sqrt{1-\alpha_c^2}}{3+\alpha_c}p_L\cos\Delta_1\cos\phi_2, \tag{24}$$

$$\frac{dN}{d\phi_4} \propto 1-\frac{\pi^2}{16}\alpha_{\Omega_c}\alpha_\Lambda\sqrt{1-\alpha_{\Omega^-}^2}\cos(\Delta_3+\phi_4). \tag{25}$$

The distributions of θ_2 and ϕ_3 are flat. The distributions in Eqs. (20) and (21) are used for fitting the values of parameters α_c and α_{Ω_c}. The distributions of ϕ_1, ϕ_2, and ϕ_4 are no longer flat when the beams are polarized trans-

versely or longitudinally. The plot for ϕ_1 distribution in Eq. (23) is given in Fig. 6, where the fluctuation is not affected by longitudinal polarization of electron beam but enhanced by the transverse polarization as plotted in Fig. 7. Conversely, the ϕ_2 distribution is free of the value of p_T but depends on longitudinal polarization p_L.

Theoretical predictions for the asymmetry parameter α_{Ω_c} are currently lacking. However, for the decays $\Xi_c^+ \to \Xi^0\pi^+$ and $\Xi_c^0 \to \Xi^-\pi^+$, which involve similar diagrams to those in Fig. 2 but with the spectator s quark replaced by a u or d quark, the absolute values of the corresponding asymmetry parameters are predicted to be around 0.95 and 0.7 [44−49], respectively. These values are used in the following analysis and should be verified at the STCF via Eq. (21). On the other hand, no measurement of the relevant parameter for $\Xi_c^+ \to \Xi^0\pi^+$ is currently available, and it will be accessible at the future STCF.

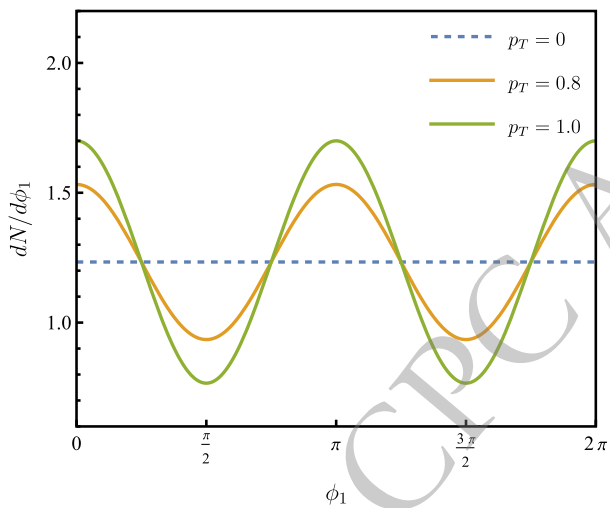

Fig. 6. (color online) The distributions of ϕ_1 for three different transverse polarizations of beam.

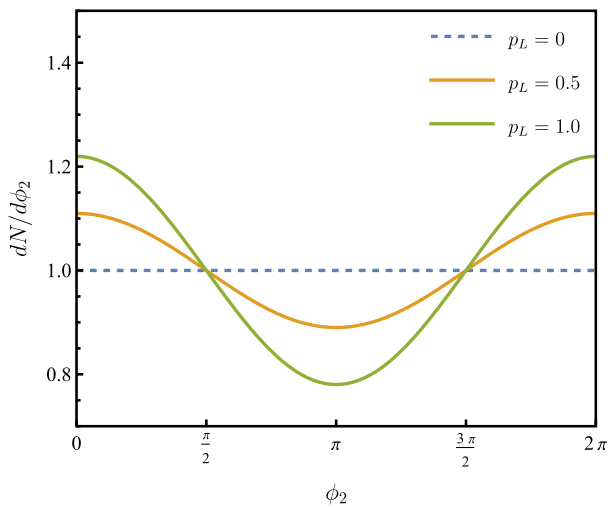

Fig. 7. (color online) The distributions of ϕ_2 for different longitudinal polarizations of electron beam. The normalization is arbitrary. Here $\alpha_{\Omega_c} = 0.7$ is used.

The joint angular distributions of θ_1 and ϕ_1 are obtained by integrating out all angles of two-body decays, and have the expression:

$$\mathcal{W}(\theta_1,\phi_1) = -\frac{64\pi^3\mathcal{P}_0}{(1+\alpha_{\Omega_c})(1+\alpha_{\Omega^-})(1+\alpha_\Lambda)}. \tag{26}$$

Since the unpolarized operator $\mathcal{P}_0$ in Eq. (11) depends on the beam polarization, the statistically measured polarization observables are also affected by the values of p_L and p_T. The measurements can be quantified by the weighted polarizations of Ω_c defined via

$$\langle\mathcal{P}_i\rangle = \int \mathcal{P}_i\mathcal{W}(\theta_1,\phi_1)\,d\cos\theta_1 d\phi_1, \tag{27}$$

where $i \in \{0,x,y,z\}$. Explicitly, the expressions of the weighted distributions for $\cos\theta_1$ or ϕ_1 are

$$\frac{d\langle\mathcal{P}_0\rangle}{d\cos\theta_1} \propto 1 + 2\alpha_c\cos^2\theta_1 + \alpha_c^2\left(\cos^4\theta_1 + \frac{p_T^4}{2}\sin^4\theta_1\right), \tag{28}$$

$$\frac{d\langle\mathcal{P}_x\rangle}{d\cos\theta_1} \propto p_L\sin\theta_1, \tag{29}$$

$$\frac{d\langle\mathcal{P}_z\rangle}{d\cos\theta_1} \propto p_L\cos\theta_1, \tag{30}$$

$$\frac{d\langle\mathcal{P}_y\rangle}{d\cos\theta_1} \propto \sin\theta_1\cos\theta_1, \tag{31}$$

$$\frac{d\langle\mathcal{P}_0\rangle}{d\phi_1} \propto 1 + \frac{2\alpha_c}{3}\left(1 + 2p_T^2\cos 2\phi_1\right) + \frac{\alpha_c^2}{5}(1 + 2p_T^2\cos 2\phi_1)^2, \tag{32}$$

$$\frac{d\langle\mathcal{P}_x\rangle}{d\phi_1} \propto p_L - p_T^2\tan\Delta_1\sin 2\phi_1, \tag{33}$$

where the factor p_L is retained for the distributions that have terms depending on p_L. Except $\cos\theta_1$ distribution of $\langle\mathcal{P}_0\rangle$ or $\langle\mathcal{P}_y\rangle$, other distributions are fluctuating only when the beams are polarized. The plots for Eqs. (28), (32) and (33) for different beam polarizations are given in Fig. 8, respectively. The ϕ_1 distributions for weighted $\mathcal{P}_y$ and $\mathcal{P}_z$ are trivially zero. Furthermore, the values of p_L and Δ_1 can be determined by combining Eqs. (24) and (33) under fixed α_{Ω_c} and p_T.

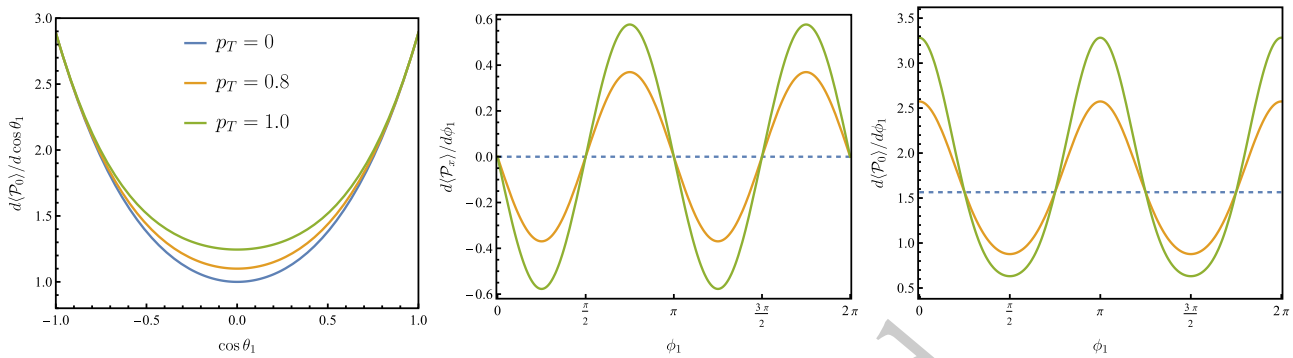

Fig. 8. (color online) Weighted polarizations of Ω_c as functions of ϕ_1 or θ_1 at different transverse beam polarizations. Here $p_L = 0$ is used.

IV. SENSITIVITY OF ASYMMETRIC PARAMETERS MEASUREMENTS

Sensitivity estimation is fundamental to experimental design, which links physical measurement precision to data statistics. We refine sensitivity estimation by using the entire decay chain for Ω_c. Our calculations show the expected precision for asymmetric parameters relative to data statistics. This method applies to similar decay processes. As large-scale facilities like STCF [26], sensitivity estimation is urgently needed to guide the plan for data collection. Currently, the STCF detector and offline software system are in the research and development stage. Therefore, according to the design report [26], the reconstruction efficiency of this process is estimated to be 30%. We can discuss whether the facility could confirm or exclude certain theoretical scenarios after considering the impacts of the branching fractions and reconstruction efficiencies.

Our estimation is based on maximum likelihood method. For the observed data sample of N events, the likelihood function is expressed as [50]

$$L(\theta_i, \phi_i, \alpha_c, \alpha_{\Omega_c}, \alpha_{\Omega^-}, \alpha_\Lambda) = \prod_{i=1}^{N} \widetilde{\mathcal{W}}_j, \tag{34}$$

where θ_i and ϕ_i represent polar angle and azimuth angle. The function depends on relative decay parameters $\alpha_c, \alpha_{\Omega_c}, \alpha_{\Omega^-}, \alpha_\Lambda$ and is computed based on the probability of the i-th event $\widetilde{\mathcal{W}}_j$, whose distribution is normalized. Then the relative uncertainty for estimating statistical sensitivity to parity parameter α_{Ω_c} is defined as

$$\delta(\alpha_{\Omega_c}) = \frac{\sqrt{V(\alpha_{\Omega_c})}}{|\alpha_{\alpha_{\Omega_c}}|}, \tag{35}$$

where the inverse of the variance is given by

$$V^{-1}(\alpha_{\Omega_c}) = N \int \frac{1}{\widetilde{\mathcal{W}}} \left[\frac{\partial \widetilde{\mathcal{W}}}{\partial \alpha_{\Omega_c}}\right]^2 \prod_i^4 d\cos\theta_i d\phi_i, \tag{36}$$

where the N denotes the number of observed events [50]. We consider a set of possible values of α_{Ω_c} to plot their sensitivities shown in Fig. 9. At a fixed number of events, the statistical sensitivity is a monotonically decreasing function of the absolute value of the asymmetry parameter. The phases $\Delta_2 = \pi/4$ and $\Delta = \pi/3$ are employed here, and other sets of phase angle values do not significantly affect the statistical quantities.

We are particularly interested in the dependence of statistical sensitivities on asymmetry parameters and beam polarizations. The distributions of $\delta(\alpha_{\Omega_c})$ for four choices of the beam polarizations are plotted in Fig. 10 with α_{Ω_c} fixed at 0.7. The sensitivity improves as its value decreases by approximately 10% when the beam is transversely polarized at $p_T = 1$ compared to an unpolarized scenario, and the value decreases by approximately 34% when the beam is longitudinally polarized at $p_L = 1$.

Indeed for identifying significance of CP violations, the statistical sensitivity of $\mathcal{A}_{CP}$ in Eq. (6) can be estimated if α_{Ω_c} and $\bar{\alpha}_{\bar{\Omega}_c}$ are considered as non-correlation, via error propagation formula:

$$\delta(\mathcal{A}_{CP}) = \frac{2\sqrt{\alpha_{\Omega_c}^2 \delta(\bar{\alpha}_{\bar{\Omega}_c})^2 + \bar{\alpha}_{\bar{\Omega}_c}^2 \delta(\alpha_{\Omega_c})^2}}{(\alpha_{\Omega_c} - \bar{\alpha}_{\bar{\Omega}_c})^2}, \tag{37}$$

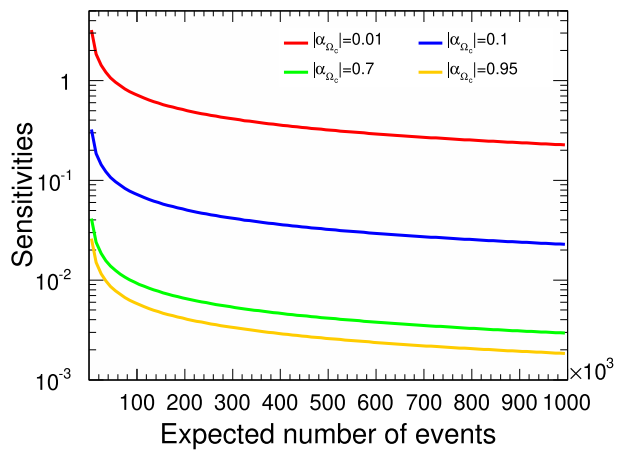

Fig. 9. (color online) The α_{Ω_c} sensitivity distributions relative to signal yields in terms of three different values.

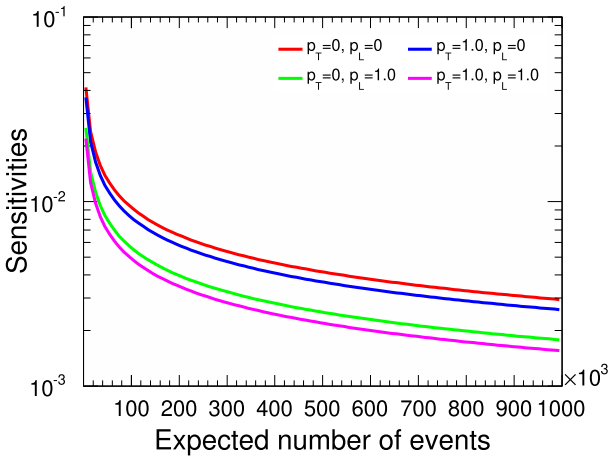

Fig. 10. (color online) The α_{Ω_c} sensitivity distributions relative to signal yields in terms of different beam polarizations.

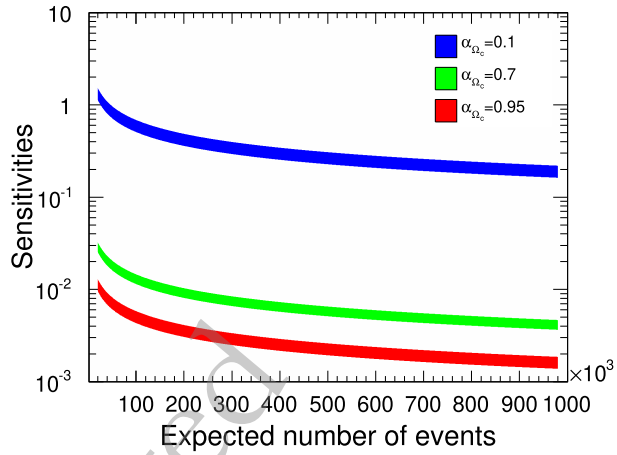

Fig. 11. (color online) The $\mathcal{A}_{CP}$ sensitivity distributions relative to signal yields in terms of two different values of α_{Ω_c}. The uncertainty from CP parameter is $|\mathcal{A}_{CP}| < 0.076$.

where $\delta(\bar{\alpha}_{\bar{\Omega}_c})$ is the sensitivity for $\bar{\Omega}_c$ system. The plots for sensitivity $\delta(\mathcal{A}_{CP})$ is shown in Fig. 11 with choosing three different values of α_{Ω_c}. The sensitivity and the CP parameter are positively correlated when other variables are fixed, and the bands are used to display uncertainty from variation $|\mathcal{A}_{CP}| < 0.076$. Though the direct CP violation from weak interactions for decays of charm baryons is of order 10^{-4} or less, we adopt the upper limit 0.076 from experiment [51] to involve possible enhancements from other mechanisms. The value of $\mathcal{A}_{CP}$ can be obtained by combining Eqs. (6) and (21), associated with determined $\alpha_{\bar{\Omega}_c}$ from the conjugation decay. The $\delta(\mathcal{A}_{CP})$ for four choices of the beam polarizations are plotted in Fig. 12 with α_{Ω_c} fixed at 0.7. They exhibit similar line shapes and evolutionary trends in Fig. 10.

The expected number of observed signal events each year is estimated, assuming that the cross section of $e^+e^- \to \Omega_c\bar{\Omega}_c$ is approximately equal to that of $e^+e^- \to \Lambda_c^+\bar{\Lambda}_c^-$ [52, 53]. The branching fractions of intermediate processes and detection efficiency have been considered in detailed calculation. The branching fraction of $\Omega_c \to \Omega^-\pi^+$ decay has been computed in Ref. [54–57] and the value 4.2% [54] is chosen in our analysis. The branching fractions of $\Omega^- \to \Lambda K^+$ and $\Lambda \to p\pi^-$ are taken from Particle Data Group [58]. The detection efficiency of the signal channel is roughly estimated to 30%. Therefore, the observed $\Omega_c \to \Omega^-\pi^+ \to \Lambda K^+\pi^+ \to p\pi^-K^+\pi^+$ yields are expected to ~ 0.37 million at STCF. Approximate values for α_{Ω_c}, inferred from the predicted parameters of Ξ_c^+ and Ξ_c^0 [49], can be tested at the STCF with a precision of 0.48% and 0.34% for $|\alpha_{\Omega_c}| = 0.7$ and 0.95, respectively, as shown in Figure 9. The expected CP violation in $\Omega_c \to \Omega^-\pi^+$ decay from weak interactions is on the order of 10^{-9} to 10^{-10}. Therefore, it is estimated that at least 2.0×10^{18} $\Omega_c\bar{\Omega}_c$ events are required to observe CP violation, under the assumption of $\alpha_{\Omega_c} = 0.95$. We can achieve precise measurement of decay parameter and CP parameter at STCF, but the data sample is not sufficient to observe CP violation unless some new physical contributions are made. The detailed statistical sensitivities $\delta(\alpha_{\Omega_c})$ and $\delta(\mathcal{A}_{CP})$ for different parameter assumptions are listed in Table 2.

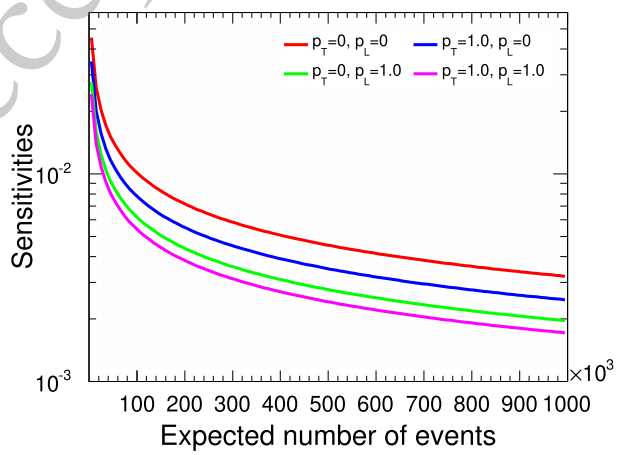

Fig. 12. (color online) The $\mathcal{A}_{CP}$ sensitivity distributions relative to signal yields in terms of different beam polarizations.

Table 2. Statistical sensitivities $\delta_{\alpha_{\Omega_c}}$ and $\delta_{\mathcal{A}_{CP}}$ for different parameter assumptions based on expected 0.37 million events. Here, $\mathcal{A}_{CP}$ is set to 0.001.

Assumed parameters	$\delta_{\alpha_{\Omega_c}}$(%)	$\delta_{\mathcal{A}_{CP}}$(%)
$\alpha_{\Omega_c} = 0.7,\ p_T = 0,\ p_L = 0$	0.48	0.49
$\alpha_{\Omega_c} = 0.95,\ p_T = 0,\ p_L = 0$	0.34	0.27
$\alpha_{\Omega_c} = 0.95,\ p_T = 1.0,\ p_L = 0$	0.28	0.22
$\alpha_{\Omega_c} = 0.95,\ p_T = 0,\ p_L = 1.0$	0.16	0.13
$\alpha_{\Omega_c} = 0.95,\ p_T = 1.0,\ p_L = 1.0$	0.14	0.10

V. SUMMARY

The beam polarization can affect the transverse and longitudinal polarization distributions of Ω_c, as well as the angular distributions of θ_1 and ϕ_1 in the center-of-mass frame of the electron-positron system. By measuring the angular distribution of the Ω_c and particles from Ω_c decay, we can infer the contributions of the transverse and longitudinal polarization of the electron-positron beam. Although both longitudinal and transverse beam polarizations can improve the precision of decay parameters and CP parameters, the longitudinal polarization exhibits greater sensitivity than the transverse polarization.

Currently, experiments have achieved preliminary control of beam polarization. For future studies, particularly in precision CP measurements, achieving controllable transverse and longitudinal polarization with high polarization ratio will be crucial. In this study, we evaluate the sensitivities of the asymmetry parameters and CP violation in the decay $\Omega_c \to \Omega^-\pi^+$ under various data sample sizes and beam polarization conditions. If the decay parameter itself is larger, the sensitivity will be better, which means that an accurate result can be measured experimentally. The polarization-dependent angular distributions and sensitivity estimates developed in this work can be used to enhance the verification of various theoretical predictions for related decays such as $\Xi_c^+ \to \Xi^0\pi^+$ and $\Xi_c^0 \to \Xi^-\pi^+$ at the STCF. This work represents the first investigation of P and CP violation in the two-body decay of Ω_c, providing essential theoretical support for future experiments, such as STCF.

References

[1] A. D. Sakharov, Pisma Zh. Eksp. Teor. Fiz. **5**, 32 (1967)
[2] N. Cabibbo, Phys. Rev. Lett. **10**, 531 (1963)
[3] M. Kobayashi and T. Maskawa, Prog. Theor. Phys. **49**, 652 (1973)
[4] A. Abashian *et al*. [Belle], Phys. Rev. Lett. **86**, 2509 (2001)
[5] B. Aubert *et al*. [BaBar], Phys. Rev. Lett. **86**, 2515 (2001)
[6] Y. Chao *et al*. [Belle], Phys. Rev. Lett. **93**, 191802 (2004)
[7] B. Aubert *et al*. [BaBar], Phys. Rev. Lett. **93**, 131801 (2004)
[8] R. Aaij *et al*. [LHCb], Phys. Rev. Lett. **122**(21), 211803 (2019)
[9] R. Aaij *et al*. [LHCb], Phys. Rev. Lett. **134**, 101802 (2025)
[10] R. Aaij *et al*. [LHCb], Nature **643**, 1223 (2025)
[11] M. Ablikim *et al*. [BESIII], Phys. Rev. Lett. **129**(13), 131801 (2022)
[12] M. Ablikim *et al*. [BESIII], Phys. Rev. Lett. **131**(19), 191802 (2023)
[13] M. Ablikim *et al*. [BESIII], Phys. Rev. Lett. **135**(14), 141804 (2025)
[14] M. Ablikim *et al*. [BESIII], Phys. Rev. D **108**(3), L031106 (2023)
[15] M. Ablikim *et al*. [BESIII], Nature **606**(7912), 64 (2022)
[16] M. Ablikim *et al*. [BESIII], Phys. Rev. Lett. **132**(10), 101801 (2024)
[17] X. G. He, J. Tandean and G. Valencia, Sci. Bull. **67**, 1840 (2022)
[18] H. Y. Cheng and B. Tseng, Phys. Rev. D **48**, 4188 (1993)
[19] J. G. Körner, G. Kramer and J. Willrodt, Phys. Lett. B **78**, 492 (1978)
[20] J. G. Korner and M. Kramer, Z. Phys. C **55**, 659 (1992)
[21] M. A. Ivanov, J. G. Korner, V. E. Lyubovitskij and A. G. Rusetsky, Phys. Rev. D **57**, 5632 (1998)
[22] H. Y. Cheng and B. Tseng, Phys. Rev. D **46**, 1042 (1992)
[23] K. K. Sharma and R. C. Verma, Eur. Phys. J. C **7**, 217 (1999)
[24] T. Uppal, R. C. Verma and M. P. Khanna, Phys. Rev. D **49**, 3417 (1994)
[25] T. D. Lee and C. N. Yang, Phys. Rev. **108**, 1645 (1957)
[26] M. Achasov *et al*., Front. Phys. (Beijing) **19**(1), 14701 (2024)
[27] S. Zeng, Y. Xu, X. R. Zhou, J. J. Qin and B. Zheng, Chin. Phys. C **47**(11), 113001 (2023)
[28] X. Cao, Y. T. Liang, and R. G. Ping, Phys. Rev. D **110**, 014035 (2024)
[29] S. U. Chung, (1971), 10.5170/CERN-1971-008.
[30] Y. C. Chen *et al*. [HyperCP], Phys. Rev. D **71**, 051102 (2005)
[31] M. Ablikim *et al*. [BESIII], Phys. Rev. Lett. **133**(10), 101902 (2024)
[32] J. P. Wang and F. S. Yu, Phys. Lett. B **849**, 138460 (2024)
[33] J. F. Donoghue, X. G. He and S. Pakvasa, Phys. Rev. D **34**, 833 (1986)
[34] M. Beneke, G. Buchalla, M. Neubert and C. T. Sachrajda, Nucl. Phys. B **591**, 313 (2000)
[35] M. Beneke, G. Buchalla, M. Neubert and C. T. Sachrajda, Nucl. Phys. B **606**, 245 (2001)
[36] H. Y. Cheng, C. K. Chua and A. Soni, Phys. Rev. D **71**, 014030 (2005)
[37] M. Saur and F. S. Yu, Sci. Bull. **65**, 1428 (2020)
[38] J. Tandean and G. Valencia, Phys. Rev. D **67**, 056001 (2003)
[39] J. P. Wang, Q. Qin and F. S. Yu, [arXiv: 2411.18323 [hep-ph]].
[40] M. G. Doncel, P. Mery, L. Michel, P. Minnaert and K. C. Wali, Phys. Rev. D **7**, 815 (1973)
[41] H. Chen and R. G. Ping, Phys. Rev. D **102**, 016021 (2020)
[42] M. Ablikim *et al*. [BESIII], Phys. Lett. B **770**, 217 (2017)
[43] N. Salone, P. Adlarson, V. Batozskaya, A. Kupsc, S. Leupold and J. Tandean, Phys. Rev. D **105**(11), 116022 (2022)
[44] P. Zenczykowski, Phys. Rev. D **50**, 5787 (1994)
[45] Z. P. Xing, X. G. He, F. Huang and C. Yang, Phys. Rev. D **108**(5), 5 (2023)
[46] H. Zhong, F. Xu, Q. Wen and Y. Gu, JHEP **02**, 235 (2023)
[47] Z. P. Xing, Y. J. Shi, J. Sun and Y. Xing, Eur. Phys. J. C **84**(10), 1014 (2024)
[48] H. Zhong, F. Xu and H. Y. Cheng, Phys. Rev. D **109**(11), 114027 (2024)
[49] P. Y. Niu, Q. Wang and Q. Zhao, Phys. Rev. D **111**(9), 093004 (2025)
[50] T. Z. Han, R. G. Ping, T. Luo, and G. Z. Xu, Chin. Phys. C

44, 013002 (2020)
[51] Y. B. Li *et al*. [Belle], Phys. Rev. Lett. **127**(12), 121803 (2021)
[52] M. Ablikim *et al*. [BESIII], Phys. Rev. Lett. **131**(19), 191901 (2023)
[53] M. Ablikim *et al*. [BESIII], Phys. Rev. D **109**(5), 053005 (2024)
[54] H. Y. Cheng, Phys. Rev. D **56**, 2799 (1997)
[55] Y. K. Hsiao, L. Yang, C. C. Lih and S. Y. Tsai, Eur. Phys. J. C **80**(11), 1066 (2020)
[56] K. L. Wang, Q. F. Lü, J. J. Xie and X. H. Zhong, Phys. Rev. D **107**(3), 034015 (2023)
[57] S. Zeng, F. Xu and Y. Gu, Eur. Phys. J. C **85**(2), 184 (2025)
[58] S. Navas *et al*. [Particle Data Group], Phys. Rev. D **110**(3), 030001 (2024)